ORNL/TM-5095

Cy 10

Krypton Absorption in Liquid CO_2 (KALC): Campaign II in the Experimental Engineering Section Off-Gas Decontamination Facility

R. W. Glass
H. W. R. Beaujean
V. L. Fowler
T. M. Gilliam
D. J. Inman
D. M. Levins

OAK RIDGE NATIONAL LABORATORY
OPERATED BY UNION CARBIDE CORPORATION FOR THE ENERGY RESEARCH AND DEVELOPMENT ADMINISTRATION

Printed in the United States of America. Available from
National Technical Information Service
U.S. Department of Commerce
5285 Port Royal Road, Springfield, Virginia 22161
Price: Printed Copy $5.50; Microfiche $2.25

ORNL/TM-5095
UC-77

Contract No. W-7405-eng-26

KRYPTON ABSORPTION IN LIQUID CO_2 (KALC): CAMPAIGN II IN THE EXPERIMENTAL ENGINEERING SECTION OFF-GAS DECONTAMINATION FACILITY

R. W. Glass
H. W. R. Beaujean*
V. L. Fowler
T. M. Gilliam
D. J. Inman
D. M. Levins**

FEBRUARY 1976

---

*Guest scientist from West Germany. Present address: Institute for Chemische Technologie, der Kernforschungsanlage, Julich GmbH, 517 Julich, West Germany.

**Guest scientist from Australia. Present address: Chemical Technology Division, Australian Atomic Energy Commission, Research Establishment, Private Mailbag, Sutherland 2232, N.S.W. Australia.

OAK RIDGE NATIONAL LABORATORY
Oak Ridge, Tennessee 37830
operated by
UNION CARBIDE CORPORATION
for the
ENERGY RESEARCH AND DEVELOPMENT ADMINISTRATION

TABLE OF CONTENTS

KRYPTON ABSORPTION IN LIQUID CO_2 (KALC): CAMPAIGN II IN THE EXPERIMENTAL ENGINEERING SECTION OFF-GAS DECONTAMINATION FACILITY

R. W. Glass
H. W. R. Beaujean
V. L. Fowler
T. M. Gilliam
D. J. Inman
D. M. Levins

ABSTRACT

Results are presented for the second major campaign for quantifying krypton removal from simulated High-Temperature Gas-Cooled Reactor reprocessing off-gas by the KALC process. The Experimental Engineering Section Off-Gas Decontamination Facility used in the campaign provides engineering-scale experiments with nominal gas and liquid flows of 5 scfm and 0.5 gpm respectively.

Equilibrium and nonequilibrium mass transfer experiments for the CO_2-O_2-Kr system are described, and a detailed discussion of the data analysis is included. The analysis, although not rigorous, is reasonable and indicates values of HTU for krypton on the order of 0.4 ft for decontamination factors from 100 to 10,000. Recent flooding information for the packed columns is combined with previous data and is shown to be well represented by an empirical flooding equation.

---

1. INTRODUCTION

As part of the Thorium Utilization Program developmental work being carried out at ORNL, the Experimental Engineering Section Off-Gas Decontamination Facility (EES-ODF, see Fig. 1) was operated to quantify the absorption of krypton by liquid CO_2.

The facility and general processing objectives have been discussed previously;[1] therefore, the present report will deal specifically with these items only as they relate to the recently completed (February 28, 1975) operations. These operations are collectively and programmatically

ORNL DWG 73-2511

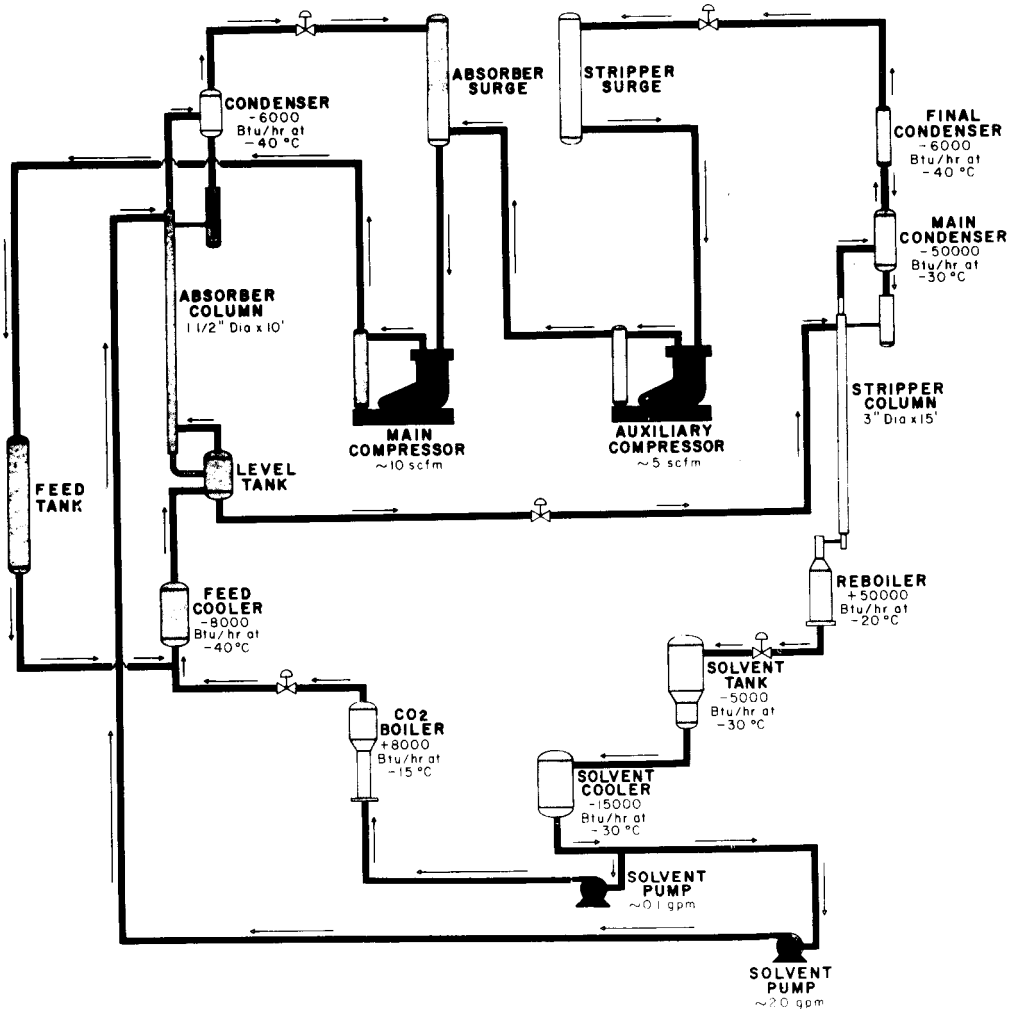

Fig. 1. Experimental Engineering Section Off-Gas Decontamination Facility.

referred to as Campaign II. Previous activities in the EES-ODF (Campaign I)[2] were, of necessity, preliminary in nature. Campaign II was comprised of approximately 30 experiments involving the mass transfer of krypton into liquid CO_2 in the presence of O_2, and 10 experiments where conditions within the packed absorption column were chosen such that CO_2-Kr equilibrium values were obtained as a check on values of equilibrium data reported in the literature.[3,4] Additional column flooding data are also presented and compared with previous values.[2]

2. FLOODING STUDIES

Fluid dynamic data for the EES-ODF packed columns have been reported.[2] More recently, a few additional experiments with the liquid CO_2 system were conducted during a High-Temperature Gas-Cooled Reactor (HTGR) campaign in the Oak Ridge Gaseous Diffusion Plant (ORGDP) facility for off-gas decontamination studies.[5]

Figure 2 presents the collective flooding information obtained for the packed columns investigated. Included in the data shown in this figure are flooded conditions found for the 1-1/2-in. absorber column and the 3-in. stripper column in the EES-ODF, together with the more recent data (darkened points) acquired from operation of the 3-in. fractionator column in the ORGDP facility. All columns are packed with presized canisters (6 in. long) of Goodloe* wire mesh packing.

---

*A product of the Packed Column Co., a Division of Metex Corp., Edison, N.J.

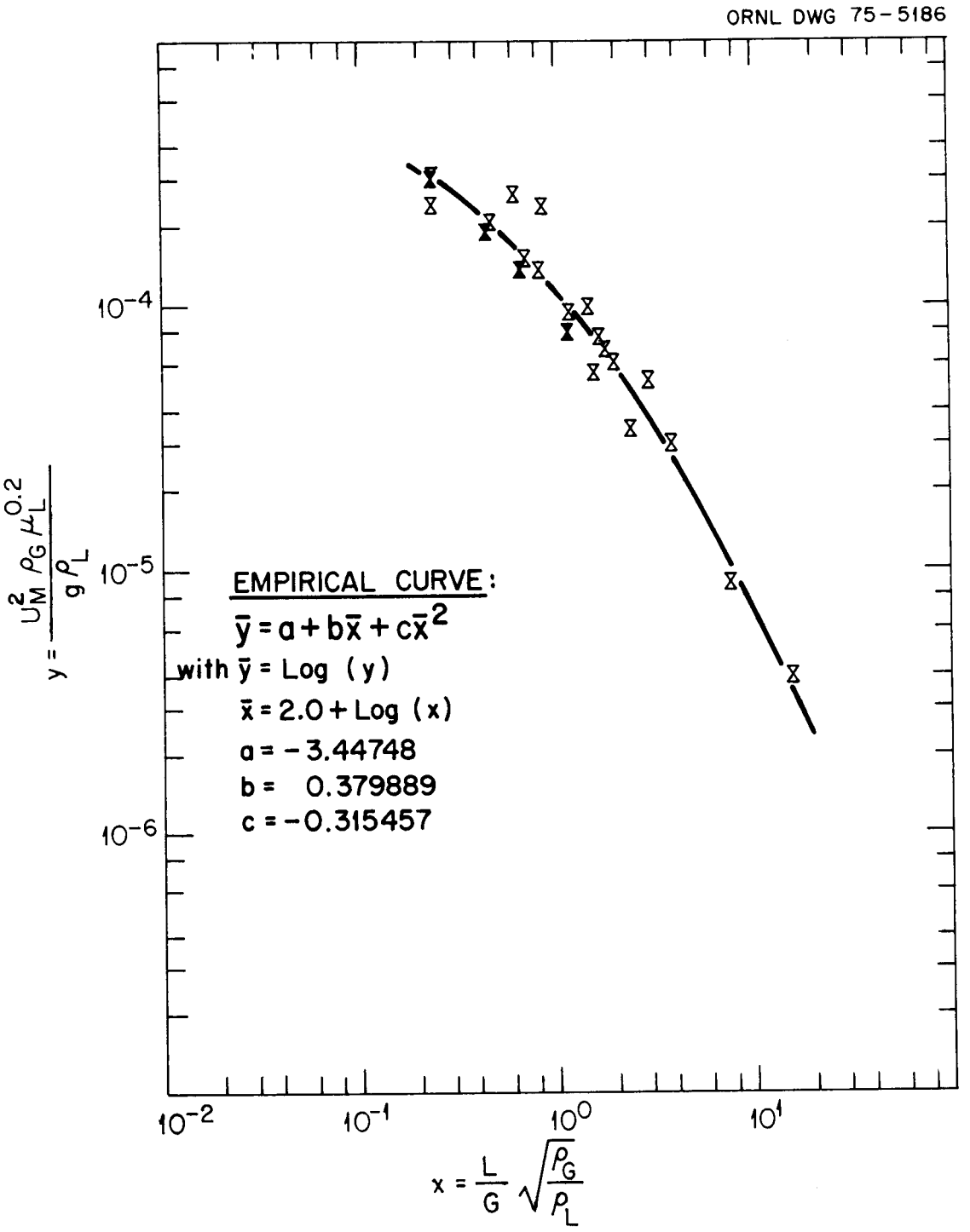

Fig. 2. Curve constructed by using collective flooding information.

The flooding curve is presented in a standard form for the particular packing (i.e., no "packing factor" is included in the ordinate grouping). The following quantities are noted for Fig. 2:

L = liquid flow rate, $lb/ft^2 \cdot hr$,

G = gas flow rate, $lb/ft^2 \cdot hr$,

ρ_G = gas-phase density, lb/ft^3,

ρ_L = liquid-phase density, lb/ft^3,

μ_L = liquid-phase viscosity, cP,

U_M = gas velocity at flooding, ft/sec,

g = 32.2 ft/sec^2.

With the addition of the four experimental points from the ORGDP fractionator, a curve has been fitted to all points shown. The results are as follows:

$$\bar{y} = a + b\bar{x} + c\bar{x}^2 = \log (y),$$

where

$\bar{x} = 2.0 + \log (x)$,

y = ordinate values of $\dfrac{U_M^2 \, \rho_G \, \mu_L^{0.2}}{g \, \rho_L}$,

x = abscissa values of $\dfrac{L}{G}\sqrt{\dfrac{\rho_G}{\rho_L}}$,

$a = -3.44748$,

$b = 0.379889$,

$c = -0.315457$.

Practically all of the fluid dynamic experiments represented by the flooding curve have involved CO_2 only (i.e., both gas and liquid phases are essentially pure CO_2). The effect of light gases such as O_2, N_2, etc., is not experimentally implicit. However, most of the areas of concern in the KALC process involve pure CO_2.

The capacity or throughput of the packing at flooding is less than that suggested in literature supplied by the vendor (overall, by perhaps 50% depending on conditions). The pressure drop at flooding is approximately 0.5 in. H_2O per foot of packing.

Examination (x-ray, etc.) of the EES-ODF absorber indicated that at some point after fabrication and installation, the packing canisters shifted, were compressed, or in certain instances even became separated from neighboring canisters. Hold-down grids in the EES-ODF stripper column appear to have prevented packing movement; however, no information on packing quality and uniformity is available for the ORGDP facility columns. Most of the experimental points shown in Fig. 2 were obtained on the 3-in. EES-ODF stripper column;[2] and it would appear that, if the observed amount of packing movement affects flooding performance, the extent is minor in the present system.

Large and unexplainable shifts of packing which occurred in the original EES-ODF stripper column[1] very definitely compromised the performance of the column. (The original stripper section was replaced because of poor performance. Subsequent investigation revealed gross packing nonuniformity and indicated a need for precautionary examination of other EES-ODF packed sections.) In general, the collective flooding

information obtained with the three packed columns (see Fig. 2) indicates an overall agreement in performance and no apparent fabrication differences.

3. EQUILIBRIUM OPERATIONS

From the beginning of Campaign II, it was recognized that a fundamental question concerning Kr-CO_2 equilibrium existed. The problem can be explained by referring to Fig. 3. Two independent sets of equilibrium data[3,4] for the same system were available, and these were not in agreement. The data are expressed as the equilibrium ratio y/x, where y and x denote krypton concentrations in the vapor and liquid CO_2 phases, respectively. Calculations based on each set of data produce widely varying results.[6] Moreoever, decisions as to what experimental conditions to use in Campaign II depended on the value of the Kr-CO_2 equilibrium ratio. Thus a series of experiments was conducted early in Campaign II to determine whether the dilemma could be resolved.

Two important considerations are worth noting. First, the EES-ODF is not designed to provide equilibrium data per se. Since the facility involves equilibrium in an indirect manner, it is a question of precision regarding the worth of equilibrium observations. Second, the degree of accuracy relative to sampling and analysis is very difficult to establish, especially in limited-time operations. Consequently, the objective of the equilibrium studies was to present evidence as to which set of equilibrium data was more nearly accurate. The

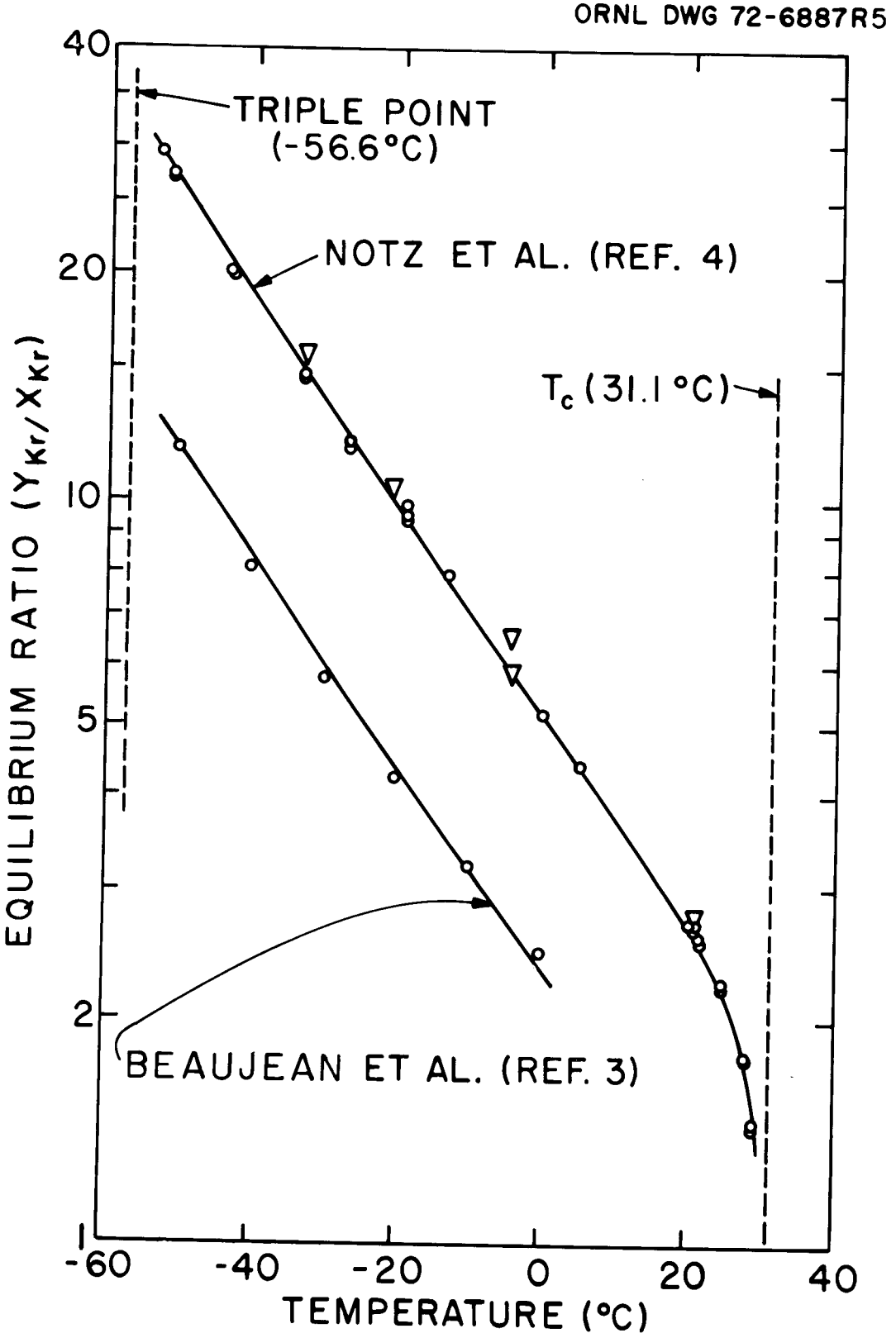

Fig. 3. Comparison of Kr-CO_2 equilibrium ratios from two independent sources.

studies also allowed a pseudo-quantitative evaluation of sampling and analytical techniques for the EES-ODF. Details of the sampling, monitoring, and analytical techniques for the EES-ODF are presented elsewhere.[7]

Table 1 presents the basic data for the ten equilibrium experiments. The method of operation during these experiments was straightforward. The facility was operated with varying amounts of oxygen, at different pressures and temperatures, but always with the liquid-to-vapor flow ratio in the absorber column set to produce a "pinched" condition at the bottom of the packed section. A pinched condition results when the liquid-to-vapor ratio is less than the equilibrium ratio (y/x), given sufficient packed section length. The result of operating in a pinched mode is that the vapor entering and the liquid leaving the column will be essentially in equilibrium.

Table 2 summarizes the equilibrium experiments with regard to the facility method of operation. After sufficient time had been allowed for system transients to subside in each run, both the gas and the liquid at the bottom of the packed section were sampled and analyzed for krypton and O_2. Calculated values given in Table 1 are based on the CO_2-O_2-Kr equilibrium model described in ORNL-TM-4947.[8] The equilibrium model assumes the validity of the data of Notz et al.[4] for krypton. Figures 4 and 5 present the computer model results for the equilibrium ratio and Henry's constant for the various components.

Figure 6 presents summary results of the equilibrium studies. Values of y and x (mole fraction) for krypton were determined by sampling and analysis, and the value of $(y/x)_{Kr}$ experimental was

Table 1. Summary of results obtained in ten equilibrium experiments in the EES-ODF

Experiment number	Pressure (psig)	Temperature (°C)	$\bar{y}_{O_2}$		$(y/x)_{Kr}$	
			Measured	Calculated[a]	Measured	Calculated[a]
232	340	-17.5	0.0770	0.1005	6.94	7.74
241	254	-28.5	0.1510	0.1537	9.02	10.23
254	375	-12.1	0.0790	0.0534	6.90	7.00
268	309	-18.5	0.0338	0.0579	8.31	8.49
275-A	338	-13.5	~0	0.0103	7.17	7.75
275-B	280	-19.6	~0	0.0130	8.72	9.33
275-C	286	-19.4	~0	0.0238	9.75	9.14
275-D	218	-27.3	~0	0.0202	11.81	11.82
275-E	290	-19.0	~0	0.0245	7.90	9.02
296	290	-25.7	(0.1180)	0.1738	8.85	9.03

[a]Calculations were based on the CO_2-Kr-O_2 model presented in ORNL-TM-4947.[8] The $(y/x)_{Kr}$ ratio was calculated assuming the validity of the data of Notz et al.[4]

Table 2. Summary of experimental equilibrium operations

Experiment number	Description of operation
232	Typical mass transfer experiment involving both gas and liquid countercurrent operation with a low value of liquid-to-vapor ratio
241	Similar to 232
254	Similar to 232
268	Similar to 232
275-A	Only liquid flow in operation; equilibrium with overgas achieved by long-term system operation
275-B	Similar to 275-A
275-C	Similar to 275-A
275-D	Similar to 275-A
275-E	Similar to 275-A
296	Similar to 232

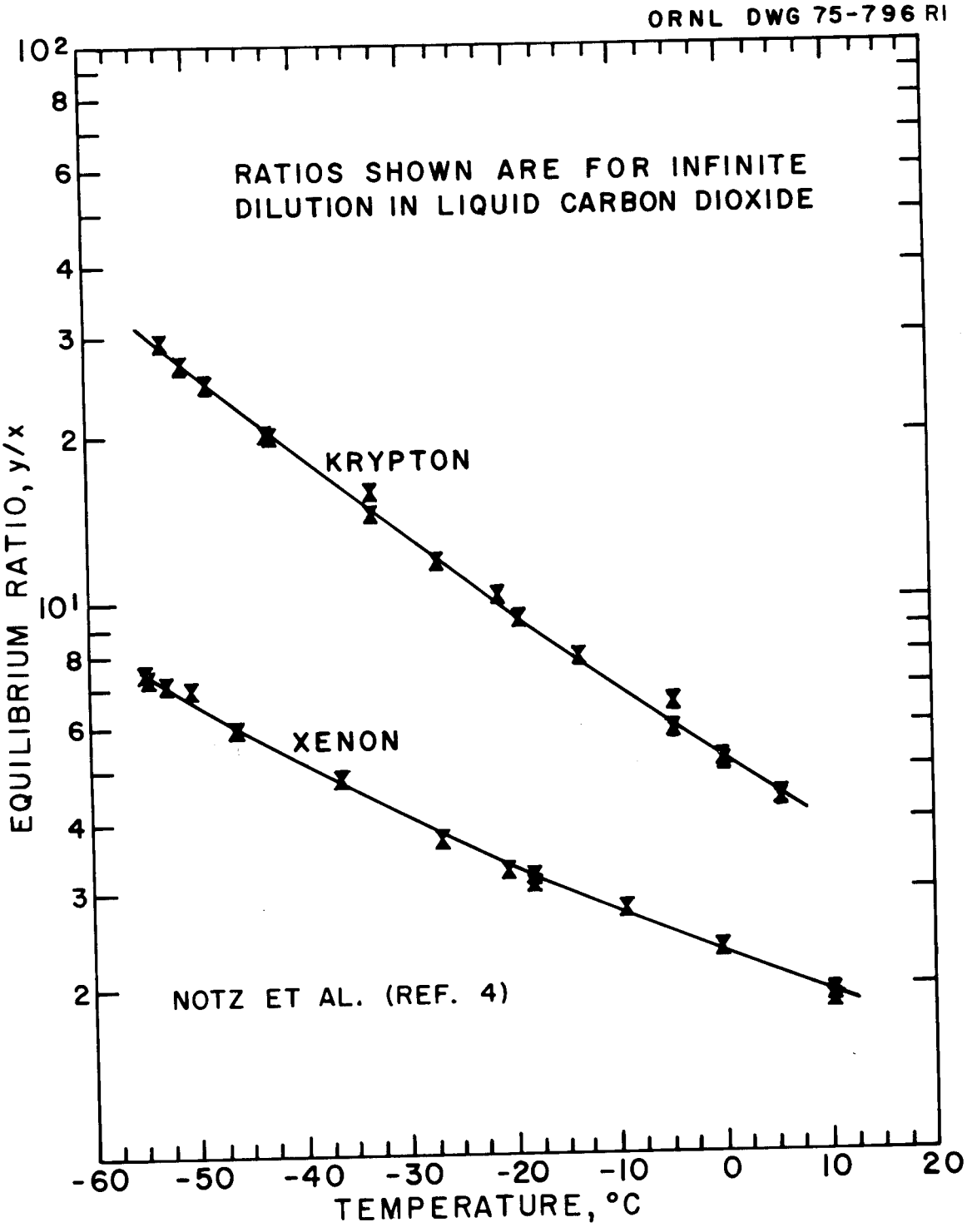

Fig. 4. Krypton and xenon equilibrium ratios as obtained by the computer model.

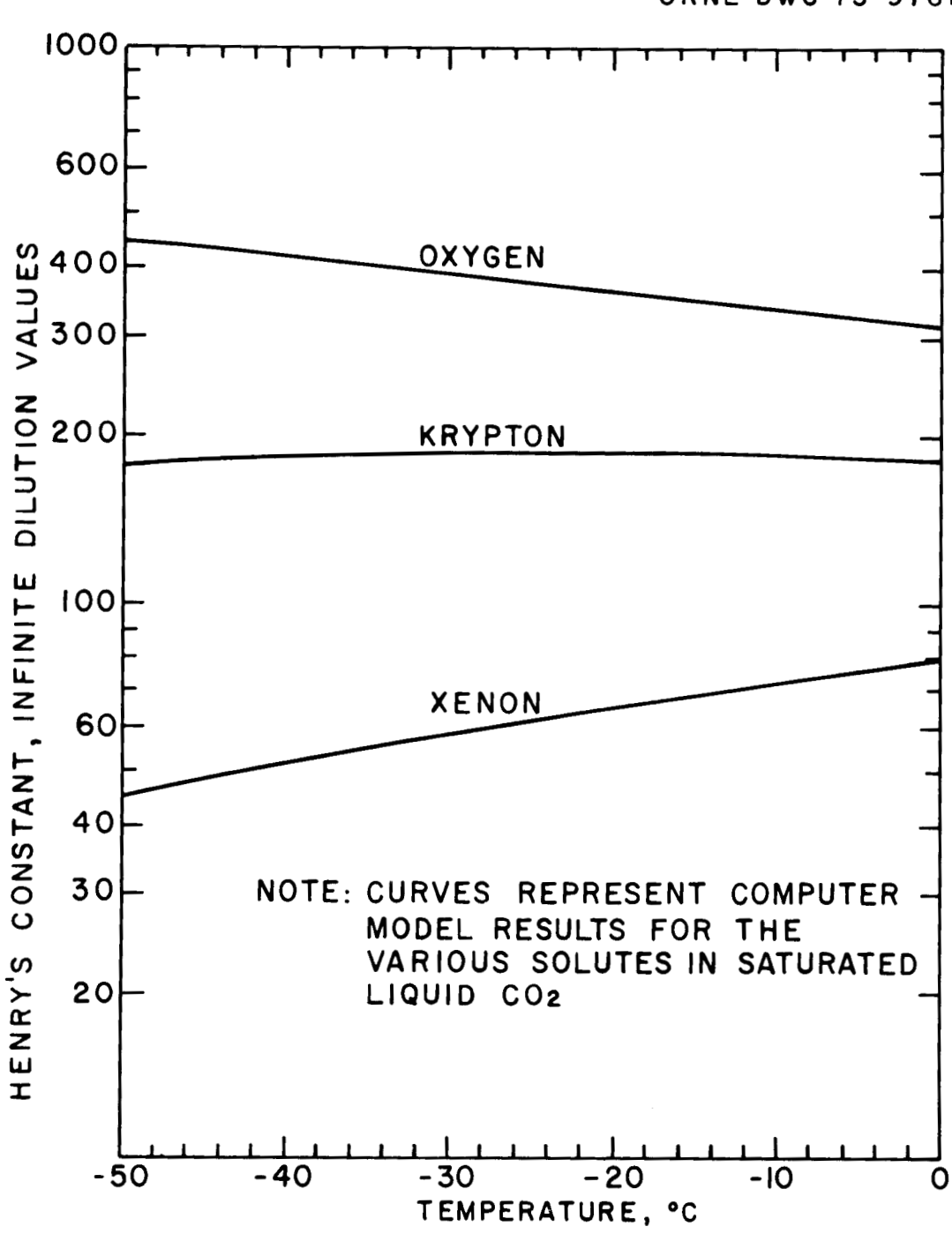

Fig. 5. Values of Henry's constant for selected solutes as obtained by the computer model.

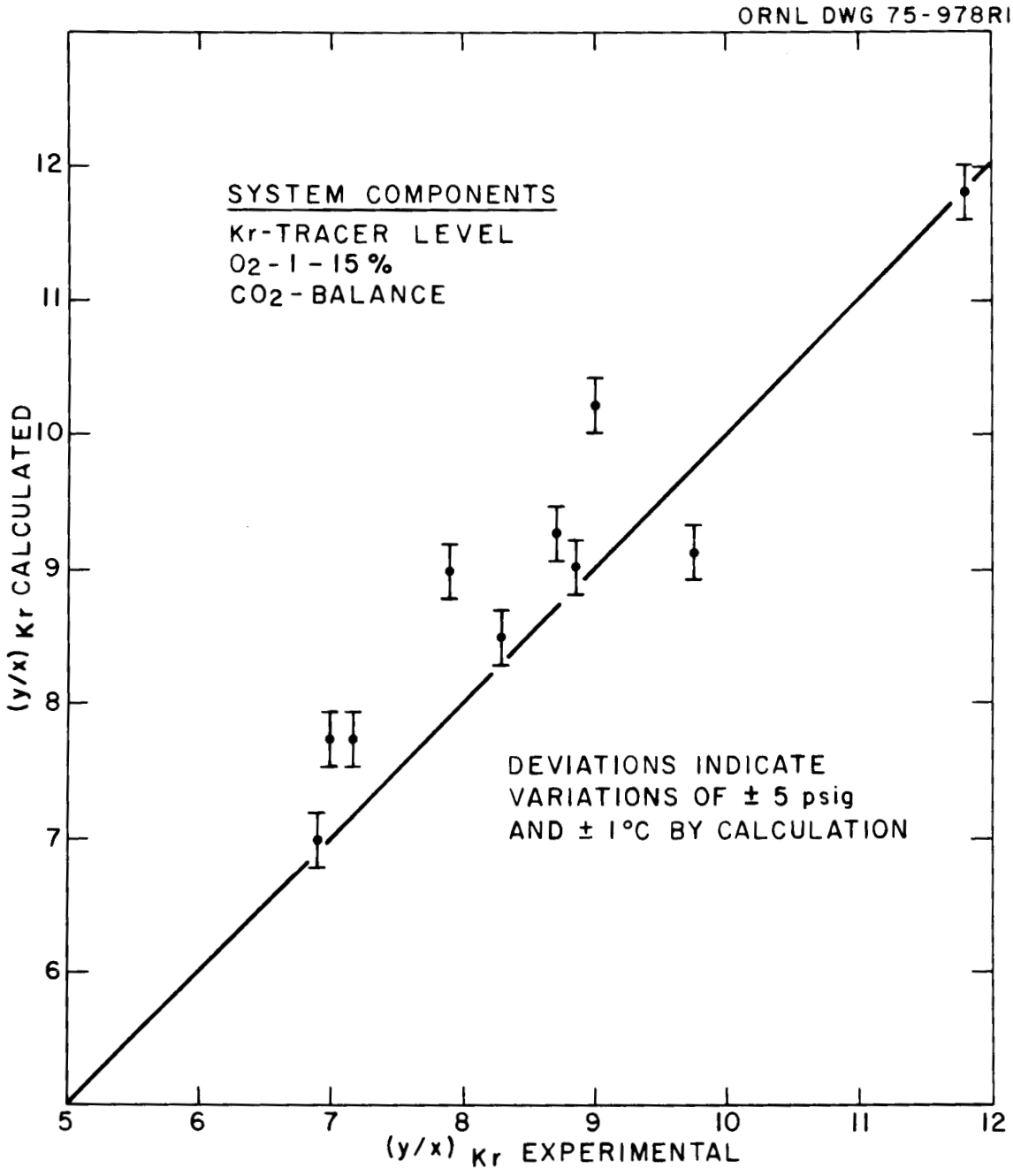

Fig. 6. Comparison of predicted and measured values of $(y/x)_{Kr}$ for the equilibrium experiments.

obtained directly. For each experimental value of P (total pressure) and T (system temperature at the bottom of the absorber), the computer model for the CO_2-Kr-O_2 equilibrium provided a corresponding value of $(y/x)_{Kr}$ calculated. Additionally, the computer model provided a value of y_{O_2} at each P and T for comparison with the measured quantity.

Considering the range of concentrations involved (< 2 mole % O_2 in the liquid and tracer-level krypton), the agreement present in Fig. 6 is remarkably good and would tend to support the data of Notz et al.[4] Thus, for the remaining experiments in Campaign II, the data of Notz et al. were assumed to be valid.

4. MASS TRANSFER EXPERIMENTS

During the mass transfer experiments carried out in Campaign II, the EES-ODF was operated in total recycle with approximately 10% light gas (O_2) and tracer-level krypton. The simulated reprocessing off-gas stream was compressed to slightly more than the desired absorption pressure and routed to the bottom of the absorber column. In the absorber, the gas (flowing upward) was contacted with essentially pure liquid CO_2 into which both O_2 and krypton were absorbed as the liquid flowed down the packed section. The solute-laden liquid was then routed to the stripper column where the dissolved gases were distilled and released into the stripper off-gas stream. The stripper and absorber off-gases were subsequently combined to form feed gas and recycled to the compressor. Liquid leaving the stripper was recycled to the top of the absorber packed section as a continuous flow of solute-free solvent.

For each of the mass transfer experiments, an operating condition was chosen and the entire flow system was allowed time for transients to subside before sampling and data acquisition. Since the entire system was operated in total recycle, it was necessary to select certain variables for control setting, and to allow the remaining variables to adjust to the overall operation. For example, in the experiments of Campaign II, the pump rate, stripper pressure, reboiler heat load, and compressor throughput were fixed. The absorber pressure control valve was adjusted manually (i.e., set at a fixed opening during steady-state operations), and the absorber pressure was allowed to seek a steady-state value. The absorber pressure could have been controlled automatically if some other variable were free to compensate. The EES-ODF seemed to reach steady state in a reasonable time if the absorber pressure was allowed to operate as the primary compensating variable. The choice of which variables to fix during the experiments is arbitrary since all variables will (or must) be at steady state in the final analysis.

Table 3 presents a portion of the data taken during the Campaign II mass transfer experiments. No purpose is served by tabulating all the data available for each experiment. However, selected results will be presented in subsequent tables as the analysis of the experimental data is discussed.

Table 3 includes data for four experiments (viz., 232, 241, 254, and 538) which were made under pinched conditions and do not reflect the nature of the other mass transfer experiments. These four experiments simply offer a lower bound to operational mass transfer. Some

Table 3. Summary of absorber conditions during mass transfer experiments in Campaign II

Experiment number	Absorber pressure (psig)	Feed gas rate (scfm)[a]	Feed gas oxygen (%)	Average absorber temp. (°C)	Absorber ΔP (in. H_2O/ft)	Liquid flow rate (gpm)	Overall krypton DF[b]
222	324	5.44	10.35	-20.0	0.364	0.551	357.
232	340	7.09	7.08	-17.4	0.516	0.551	5.
241	254	6.19	9.42	-28.2	0.255	0.485	7.
254	375	7.22	7.79	-12.2	0.619	0.485	3.
309	302	4.65	7.13	-20.1	0.413	0.623	256.
320	308	4.56	6.82	-20.1	0.510	0.720	14039.
330	308	4.57	7.83	-20.4	0.449	0.693	4161.
340	313	4.27	8.99	-20.5	0.473	0.693	7000.
348	310	4.55	9.19	-20.3	0.668	0.748	9687.
358	313	4.73	9.28	-20.8	0.467	0.665	619.
368	321	4.81	12.60	-20.9	0.516	0.623	7206.
378	337	4.99	11.70	-20.0	0.437	0.582	3214.
388	337	4.97	11.64	-20.0	0.449	0.582	3043.
406	384	5.87	20.06	-18.8	0.461	0.554	1215.
416	387	6.21	15.14	-18.3	0.394	0.485	1013.
426	347	5.74	11.93	-20.5	0.443	0.554	153.
436	345	5.39	10.75	-19.3	0.419	0.554	539.
451	325	4.77	11.34	-20.9	0.319	0.416	590.
461	336	4.40	10.47	-19.2	0.328	0.416	2602.
470	333	3.78	8.88	-18.7	0.316	0.416	3075.
480	317	5.23	10.83	-22.2	0.307	0.416	87.
490	323	6.33	8.62	-21.9	0.327	0.416	10.
498	323	3.73	8.45	-18.9	0.303	0.416	5157.
518	405	4.50	7.57	-12.6	0.376	0.416	839.
528	402	3.63	10.05	-11.7	0.376	0.416	4038.
538	409	6.38	7.80	-11.6	0.425	0.416	5.
548	396	5.16	5.93	-12.7	0.399	0.416	17.
558	391	4.67	6.79	-13.2	0.387	0.416	100.
568	407	4.23	6.24	-11.9	0.388	0.416	1100.
578	392	3.49	6.01	-12.17	0.376	0.416	2908.

[a] scfm refers to real CO_2 gas at 70°F and 1 atm.

[b] DF = decontamination factor.

of the values listed in Table 3 were obviously not obtained directly by experiment but, instead, were calculated from more fundamental measurements. The absorber pressure, average absorber temperature, absorber ΔP, and liquid rate are shown as measured. Feed gas rates were dependent on rotameter calibrations, while the O_2 content of the feed gas and overall krypton decontamination factors (DF's) were based on sampling and monitoring. A more complete discussion of these items will be presented later in this report as details of the data analysis are considered.

4.1 System Operation During Mass Transfer Experiments

As indicated earlier, mass transfer experiments were conducted using the EES-ODF absorber and stripper columns in combination to provide absorber feed gas via complete recycle of the mixed column off-gases. Recycle of the liquid was achieved by flow to the absorber, then to the stripper, and back again to the absorber. Krypton and O_2 trapped in the absorber were desorbed by continuous stripper operation.

Numerous temperatures throughout the entire EES-ODF were recorded and used as a prime indicator of general system performance. Liquid pump rates and level indications were recorded only for the purpose of providing an additional observable performance index. Occasionally, system operations were altered by outside influences, and observations of the above parameters allowed evaluations of these disturbances and provided a basis for their corrections.

Once the facility approached the steady-state conditions, as opposed to startup conditions, the various pressure, level, and flow controllers

were fine-tuned to eliminate control-induced cycling. As various gas compositions, flow rates, heater loads, etc., were investigated, the adjustment of refrigeration expansion valves and backpressure regulators became a major part of each experiment. Such adjustments were necessary because of the varying duty imposed on the system heat exchangers. Minor variations of load would be relatively easily (and automatically) compensated for in once-through commercial operations. (As indicated here and implied throughout this report, a very real difference exists in the operation of an experimental facility, such as the EES-ODF, and a once-through complete KALC system; this difference must not be overlooked or misinterpreted.)

Numerous gas and liquid samples were taken for each experiment, and measurements were made of system temperatures, pressures, etc. In large part, these data have been retained for future analyses of a more rigorous nature, pending the development of a more comprehensive computer model.

4.2 Data Analysis

It is well known that, as the amount of data collected for a given experiment increases, the general analysis becomes more involved. At various points in the analysis, however, definite decisions must be made regarding the most expedient method to be pursued. Engineering-scale experiments generally provide data which must be tempered by experiences gained during equipment operations. For example, one recorder may be found to be more consistently reliable than another.

Certain samples may be taken more easily than others and, consequently, may deserve more consideration. Such factors have been incorporated into the data analyses that follow. As indicated earlier, it is hoped that experience gained in the present analysis may permit future analyses to be more rigorous.

4.2.1 Model identification

For the purpose of identifying the streams, a schematic representation of the EES-ODF is presented as Fig. 7. The symbols used in this figure are defined as follows:

Equipment	Stream
FGC - Feed gas cooler	1 - Absorber column feed liquid
ALT - Absorber level tank	2 - Feed gas
ABS - Absorber column	3 - Liquid leaving absorber packing
STR - Stripper column	4 - Vapor entering absorber packing
REB - Reboiler	5 - Liquid entering absorber packing
CON - Condenser(s)	6 - Vapor leaving absorber packing
	7 - Stripper feed liquid
	8 - Absorber off-gas
	9 - Stripper off-gas

It must be noted that direct measurements cannot be made on streams 3, 4, 5, and 6 (i.e., the streams entering and leaving the packed section). Unfortunately, it is precisely these streams which are most important in determining the mass transfer. In reality, stream 1 (liquid CO_2) is introduced above the packed section, and

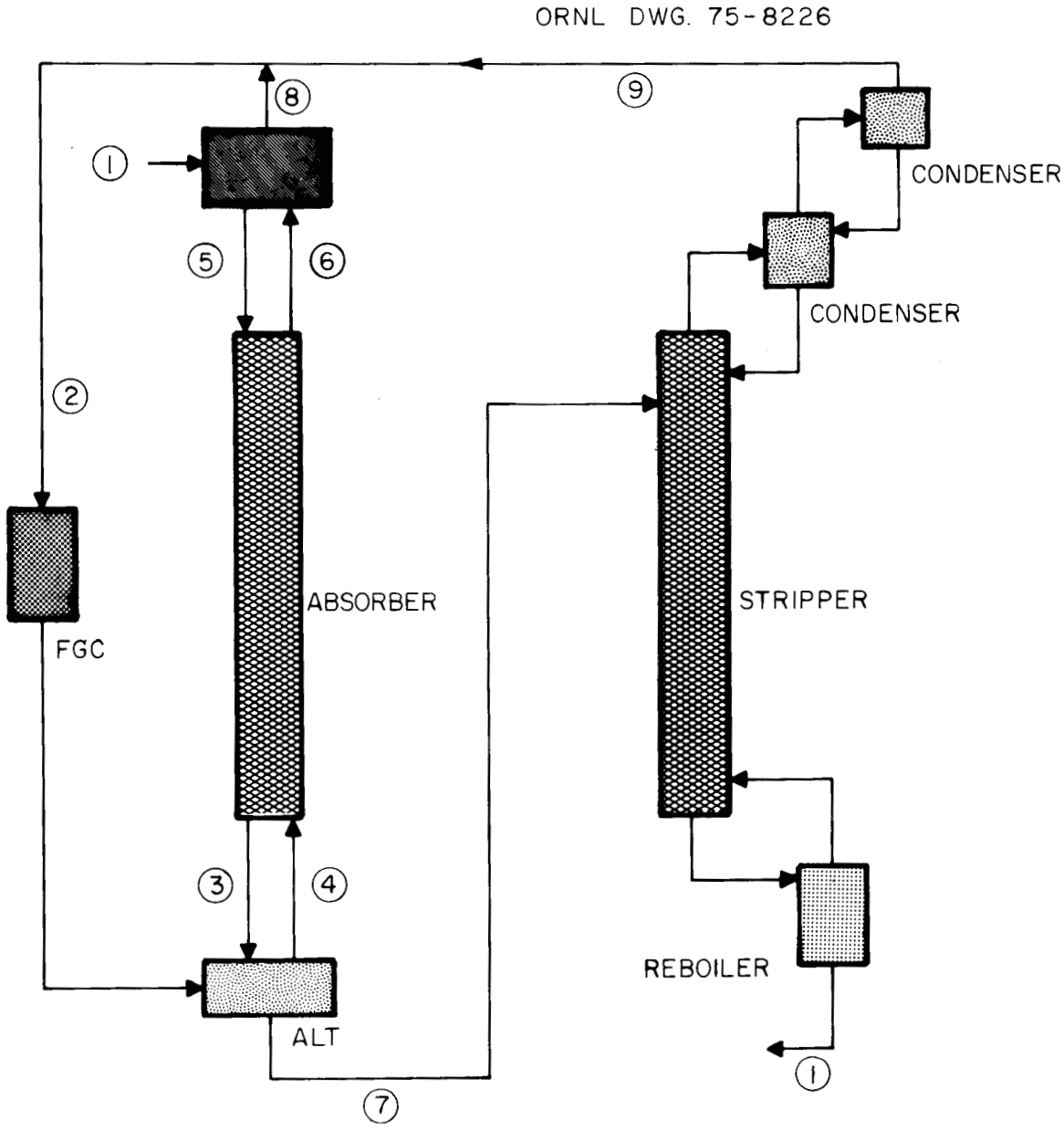

Fig. 7. Identification of EES-ODF streams for data analysis.

both heat transfer and mass transfer occur between this stream and the vapor leaving the top of the packed section (stream 6). This contacting is ascribed to the "stage" indicated above the packed section, with streams 5 and 8 resulting. Similarly, stream 2, which is the feed gas stream from system compressor, may (and generally does) undergo partial condensation in the feed gas cooler; in addition, further heat transfer and mass transfer undoubtedly occur in the absorber level tank. In reality, many of the streams considered are two-phase flows and have been idealized as homogeneous fluids only for analysis purposes.

4.2.2 Stream quantification

During Campaign II only stream 2, the feed gas stream, could be identified with respect to both flow rate (via rotameter) and composition (sampling and analysis). Off-gas streams 8 (from the absorber) and 9 (from the stripper) were sampled and analyzed for composition, but their flow rates were not known accurately since flowmeters for these streams were unreliable.

Knowledge of the compositions (O_2 and krypton) for streams 2, 8, and 9, together with flow rate values for stream 2, allows calculation of flow rates for streams 8 and 9 by two methods. If O_2 or krypton material balances together with overall stream balances are considered (note that stream 2 is simply a combination of streams 8 and 9), the following calculations are possible:

$$Q_9 = Q_2 \frac{y_2 - y_8}{y_9 - y_8} , \qquad (1)$$

$$Q_8 = Q_2 - Q_9 , \qquad (2)$$

where

Q_2 = feed gas rate, scfm,

Q_9 = stripper off-gas rate, scfm,

Q_8 = absorber off-gas rate, scfm,

y_2 = O_2 or krypton concentration in Q_2,

y_9 = O_2 or krypton concentration in Q_9,

y_8 = O_2 or krypton concentration in Q_8.

Since the quantities y_2, y_9, y_8, and Q_2 are known by measurement, Eqs. (1) and (2) represent two equations in two unknowns (Q_8 and Q_9). Determination of O_2 and krypton concentrations require both sampling and analyses of gas streams. Oxygen is analyzed by mass spectrometry, while krypton is analyzed by beta counting of the ^{85}Kr tracer. Operational experience provides more confidence in the determination of the ^{85}Kr content; therefore, the assumption of a complete krypton balance was made. Thus the y's in Eq. (1) were assumed to apply to krypton, with the result that the oxygen values in streams 2, 8, and 9 do not necessarily balance. Two reasons may be given for this "imbalance": (1) the krypton has been assumed to balance, and (2) experimental measurements are seldom of sufficient accuracy for complete overall and individual component balances to be met simultaneously. In the present analysis the inaccuracies involved in flow rate, O_2 content, and krypton content have been combined into the oxygen imbalance.

Once the stream flow rates for streams 8 and 9 have been calculated, an "oxygen balance," B, may be found from Eq. (3):

$$B = \frac{Q_8 y_8 + Q_9 y_9}{Q_2 y_2} , \qquad (3)$$

where

B = fractional O_2 balance, combined off-gas O_2 relative to feed gas O_2,

Q_2, Q_8, Q_9 = flow rates as given in Eqs. (1) and (2),

y's = oxygen concentrations for the respective streams.

For further calculational purposes, the oxygen concentrations are normalized as follows for streams 2, 8, and 9:

$$y_8^N = y_8^M (1 + 1/B)/2, \qquad (4)$$

$$y_9^N = y_9^M (1 + 1/B)/2, \qquad (5)$$

$$y_2^N = y_2^M (1 + B)/2, \qquad (6)$$

where

y's = oxygen concentrations for respective streams, with M indicating measured concentrations and N indicating normalized concentrations,

B = oxygen balance factor defined by Eq. (3).

Table 4 presents the measured and calculated quantities for streams 2, 8, and 9.

Table 4. Gas stream values for Campaign II

Experiment number	Measured ^{85}Kr concentration (ppb)			Measured O_2 concentration (%)			Measured flow rate (scfm)[a]	Calculated flow rate (scfm)		Normalized O_2 concentration (%)			O_2 balance factor
	Stream 2	Stream 8	Stream 9	Stream 2	Stream 8	Stream 9	Stream 2	Stream 8	Stream 9	Stream 2	Stream 8	Stream 9	
222	18.31	0.088	43.82	10.70	6.28	15.20	5.44	3.17	2.27	10.35	6.50	15.74	0.93
232	15.9	5.140	38.00	7.30	6.45	7.70	7.09	4.77	2.32	7.08	6.66	7.95	0.94
241	3.28	0.653	9.80	9.73	7.60	12.85	6.19	4.41	1.78	9.42	7.86	13.29	0.94
254	0.47	0.214	1.28	7.90	6.80	10.50	7.22	5.51	1.71	7.79	6.90	10.65	0.97
309	40.8	0.219	148.70	7.35	4.70	12.75	4.65	3.38	1.27	7.13	4.85	13.17	0.94
320	45.7	0.005	142.00	7.40	2.80	13.50	4.56	3.10	1.47	6.82	3.06	14.75	0.84
330	46.44	0.016	145.34	7.60	4.70	15.20	4.57	3.11	1.46	7.83	4.57	14.77	1.06
340	49.68	0.011	142.37	8.90	4.10	18.35	4.27	2.78	1.49	8.99	4.06	18.18	1.02
348	51.69	0.009	138.86	9.10	3.80	18.50	4.55	2.86	1.70	9.19	3.77	18.32	1.02
358	40.3	0.090	144.00	9.20	5.30	19.80	4.73	3.41	1.32	9.28	5.26	19.64	1.02
368	41.99	0.009	116.74	12.00	5.80	26.40	4.81	3.08	1.72	12.60	5.54	25.19	1.10
378	44.13	0.024	104.89	11.60	6.00	19.80	4.99	2.89	2.10	11.70	5.95	19.63	1.02
388	43.74	0.025	105.80	11.80	5.90	19.40	4.97	2.92	2.05	11.64	5.98	19.67	0.97
406	29.4	0.068	45.60	20.20	17.80	21.10	5.87	2.09	3.78	20.06	17.92	21.25	0.99
416	28.8	0.084	43.50	14.80	16.40	15.00	6.21	2.10	4.11	15.14	16.04	14.67	1.05
426	24.4	0.281	55.90	12.10	9.05	15.30	5.74	3.25	2.49	11.93	9.18	15.52	0.97
436	21.08	0.065	52.80	10.80	6.00	17.80	5.39	3.24	2.15	10.75	6.03	17.88	0.99
451	19.56	0.058	45.57	11.75	7.00	16.15	4.77	2.73	2.04	11.34	7.27	16.76	0.93
461	20.63	0.016	40.88	10.80	5.70	14.50	4.40	2.18	2.22	10.47	5.89	14.97	0.94
470	24.88	0.018	45.60	9.10	3.95	12.60	3.78	1.72	2.06	8.88	4.05	12.91	0.95
480	18.82	0.337	51.52	10.90	8.25	15.20	5.23	3.34	1.89	10.83	8.30	15.30	0.99
490	18.42	2.810	45.13	9.00	7.25	9.95	6.33	3.99	2.33	8.62	7.58	10.41	0.92
498	21.85	0.010	38.88	8.12	3.75	12.70	3.73	1.63	2.09	8.45	3.61	12.22	1.08
518	18.69	0.043	39.05	7.65	5.55	9.60	4.50	2.35	2.15	7.57	5.61	9.71	0.98
528	18.59	0.009	39.17	10.50	5.50	14.15	3.63	1.91	1.72	10.05	5.76	14.81	0.92
538	15.42	4.720	34.24	7.90	7.20	8.60	6.38	4.07	2.31	7.80	7.29	8.71	0.98
548	14.35	1.350	37.33	5.95	4.83	7.80	5.16	3.29	1.86	5.93	4.85	7.83	0.99
558	14.44	0.238	36.20	6.95	5.00	9.15	4.67	2.83	1.85	6.79	5.12	9.36	0.96
568	16.49	0.030	32.92	6.30	4.15	8.20	4.23	2.11	2.12	6.24	4.19	8.28	0.98
578	13.94	0.009	29.10	6.20	3.40	8.45	3.49	1.82	1.67	6.01	3.51	8.73	0.94

[a] scfm refers to 70°F, 1 atm.

To facilitate calculations, all stream flow rates have been expressed in scfm (70°F, 1 atm). This terminology is quite normal for gas flows, but liquid flows will also be referred to in terms of scfm, implying "equivalent" scfm. Actually, only stream 1, the liquid CO_2 feed to the absorber column, is involved here since the other liquid flows are calculated directly in equivalent scfm by material balance. In the case of stream 1 (pure CO_2 liquid), the flow rate in equivalent scfm is calculated as follows:

$$\text{equivalent scfm} = \frac{(\rho_L^* \text{ lb/ft}^3)\ (Q_1 \text{ gpm})}{(7.481 \text{ gal/ft}^3)(\rho_g^s \text{ lb/ft}^3)} \quad , \qquad (7)$$

where

ρ_L^* = density of saturated liquid at fluid temperature,

ρ_g^s = density of gas at standard conditions (0.114485 lb/ft^3 at 70°F, 1 atm),

Q_1 = flow rate of liquid CO_2 to the absorber, gpm.

Table 5 presents the results of these conversions for stream 1.

Flow rates for stream 7, the liquid feed to the stripper column (expressed in equivalent scfm, 70°F, 1 atm) are calculated by an overall material balance around the absorber column:

$$Q_7 = Q_1 + Q_2 - Q_8 \ . \qquad (8)$$

Values for Q_1 and Q_7 are presented in Table 5, for Q_2 (as feed gas rate) in Table 3, and for Q_8 (as calculated stream 8) in Table 4.

Table 5. Liquid flow rates for Campaign II

Experiment number	Pump rate (gpm)	Temperature (°C)	Q_1 (equivalent scfm)[a]	Q_7 (equivalent scfm)[a]
222	0.551	-26.5	42.54	44.81
232	0.551	-26.5	42.54	44.86
241	0.485	-26.7	37.46	39.24
254	0.485	-23.8	37.02	38.73
309	0.623	-28.4	48.49	49.76
320	0.720	-28.0	55.94	57.41
330	0.693	-28.5	53.89	55.35
340	0.693	-28.6	53.91	55.41
348	0.748	-29.0	58.32	60.02
358	0.665	-28.7	51.78	53.10
368	0.623	-22.7	47.39	49.11
378	0.582	-29.6	45.47	47.57
388	0.582	-30.0	45.54	47.59
406	0.554	-32.8	43.85	47.63
416	0.485	-32.2	38.28	42.39
426	0.554	-31.2	43.58	46.06
436	0.554	-28.2	43.06	45.21
451	0.416	-29.8	32.50	34.55
461	0.416	-29.8	32.50	34.72
470	0.416	-30.2	32.55	34.62
480	0.416	-29.6	32.48	34.36
490	0.416	-29.2	32.43	34.76
498	0.416	-30.3	32.57	34.66
518	0.416	-21.8	31.46	33.61
528	0.416	-21.5	31.42	33.15
538	0.416	-22.1	31.50	33.82
548	0.416	-22.0	31.49	33.35
558	0.416	-22.0	31.49	33.34
568	0.416	-22.0	31.49	33.61
578	0.416	-22.1	31.50	33.17

[a]scfm refers to 70°F, 1 atm.

Compositions for stream 7 are calculated based on the assumption that essentially all krypton and oxygen present in stream 7 report to the stripper off-gas, stream 9. Hence we obtain for both oxygen and krypton, by material balance:

$$x_7 = \frac{Q_9\, y_9}{Q_7} \quad . \tag{9}$$

Concentrations of oxygen and krypton calculated via Eq. (9) are presented in Table 6.

The overall krypton DF as presented in Table 3 is calculated from the krypton present in streams 2 (feed gas) and 8 (absorber off-gas) as follows:

$$\text{Overall DF} = \frac{Q_2\, y_2}{Q_8\, y_8} \quad . \tag{10}$$

Values of Q_2, y_2, Q_8, and y_8 are presented in Tables 3 and 4.

The calculation of packed section HTU's (or HETP's) begins with the assumption that oxygen is pinched (at equilibrium) at the bottom of the packed section. This assumption, in part, allows for the identification of streams 3 and 4. Throughout the range of temperatures and pressures encountered in Campaign II, the CO_2-O_2 equilibrium (y and x) values are extremely sensitive to temperature. Thus, since gas samples were taken from a point immediately below the absorber packed section, the additional information provided by thermocouple measurements at that point provides two means of calculating CO_2-O_2 equilibrium concentrations. Either the system pressure and temperature (to provide oxygen y and x values) or the system pressure and the measured gas-phase oxygen concentration (to provide the liquid-phase composition x

Table 6. Calculated solute concentrations in the stripper feed liquid

Experiment number	Oxygen concentration (%)	^{85}Kr concentration (ppb)
232	0.796	2.216
232	0.411	1.967
241	0.602	0.444
254	0.469	0.056
309	0.336	3.795
320	0.377	3.633
330	0.389	3.829
340	0.489	3.831
348	0.518	3.922
358	0.489	3.587
368	0.887	4.111
378	0.865	4.624
388	0.849	4.566
406	1.687	3.620
416	1.422	4.216
426	0.838	3.019
436	0.849	2.507
451	0.992	2.697
461	0.957	2.613
470	0.769	2.717
480	0.840	2.829
490	0.699	3.030
498	0.738	2.348
518	0.621	2.498
528	0.770	2.037
538	0.595	2.341
548	0.437	2.085
558	0.518	2.004
568	0.522	2.075
578	0.439	1.465

and the associated system temperature) may be used to determine the required equilibrium values. In our work, the decision was made to use the system pressure together with the measured gas-phase O_2 concentration, and the resulting equilibrium temperature was used as a check for general consistency against the measured temperature. The data of concern here are presented in Table 7. Details of the equilibrium calculational routine are presented elsewhere.[8] Table 7 shows that the calculated and measured temperatures agree quite well; hence, for consistency in further calculations, the calculated temperature was assumed. The krypton equilibrium ratios (y/x) corresponding to each calculated temperature are also shown in Table 7.

Calculations for stream rates Q_3 and Q_4 are based on overall and component (oxygen) material balances around the feed gas cooler (FGC) and the absorber level tank (ALT). Therefore,

$$Q_2 + Q_3 = Q_4 + Q_7, \tag{11}$$

$$Q_2 y_2 + Q_3 x_3 = Q_4 y_4 + Q_7 x_7. \tag{12}$$

Combining Eqs. (11) and (12) yields:

$$Q_4 = \frac{Q_2(y_2 - x_3) + Q_7(x_3 - x_7)}{y_4 - x_3}. \tag{13}$$

Compositions x_3 and y_4 for oxygen are the equilibrium values found as indicated above and presented in Table 7. Compositions y_2 (Table 4) and x_7 (Table 6) were discussed earlier, as were flows Q_2 (Table 3) and Q_7 (Table 5). If we know Q_4 [from Eq. (13)], then Q_3 can be calculated by using Eq. (11).

Table 7. Oxygen and krypton equilibrium data obtained from operating under oxygen-pinched conditions

Experiment number	Measured			Calculated		
	Pressure (psig)	Stream 4 O_2 Conc. (%)	Temp. (°C)	Temp. (°C)	Stream 3 O_2 Conc. (%)	$(y/x)_{Kr}$
222	324	14.5	-20.5	-21.1	0.910	8.12
232	340	7.7	-17.5	-16.4	0.522	7.73
241	254	15.1	-28.5	-28.4	0.714	10.23
254	375	7.9	-12.1	-13.3	0.602	7.01
309	302	7.9	-20.4	-20.2	0.466	8.69
320	308	7.5	-20.6	-19.4	0.453	8.52
330	308	8.9	-20.9	-20.0	0.536	8.52
340	313	9.1	-21.2	-19.6	0.558	8.39
348	310	8.6	-21.0	-19.7	0.522	8.47
358	313	9.3	-21.2	-19.7	0.570	8.39
368	321	14.3	-22.2	-21.3	0.888	8.20
378	337	14.8	-21.4	-20.1	0.972	7.82
388	337	14.4	-21.3	-19.9	0.947	7.82
406	384	23.5	-20.0	-20.7	1.748	6.90
416	387	22.4	-19.5	-19.9	1.685	6.85
426	347	15.2	-21.2	-19.4	1.032	7.60
436	345	14.2	-20.2	-19.1	0.960	7.64
451	325	17.2	-21.9	-22.3	1.074	8.10
461	336	15.7	-20.5	-20.6	1.024	7.85
470	333	12.5	-20.0	-19.3	0.815	7.91
480	317	16.3	-22.9	-22.6	0.992	8.30
490	323	13.1	-22.2	-20.5	0.823	8.15
498	323	12.0	-20.2	-20.0	0.756	8.14
518	405	10.1	-13.4	-11.9	0.834	6.49
528	402	12.3	-12.6	-13.3	0.998	6.56
538	409	9.5	-11.6	-11.3	0.795	6.43
548	396	7.2	-13.0	-11.2	0.587	6.63
558	391	8.4	-13.5	-12.2	0.672	6.72
568	407	8.0	-12.4	-10.7	0.672	6.45
578	392	7.6	-12.9	-11.7	0.611	6.70

Values calculated for Q_3 and Q_4 are presented, along with the liquid-to-vapor flow ratio (Q_3/Q_4) in Table 8. Except for a short length of packing at the top of the column (where practically all of the O_2 mass transfer occurs), the Q_3/Q_4 ratio was found to be a most reasonable estimate of the liquid-to-vapor flow ratio throughout the packed section. This conclusion is supported by two observations: (1) thermocouple measurements indicate that a very slight temperature gradient exists throughout the packed section; and (2) if a straight operating line is assumed to represent mass transfer along the length of the packed section and experimental values of krypton concentrations (both y and x obtained by sampling and analysis) are grouped and correlated by a least-squares technique for each experiment, the resulting line slope agrees quite well with the value of Q_3/Q_4 noted above.

Values of ^{85}Kr concentrations in streams 3 and 4 are found by a material balance around the absorber column (viz., streams 1, 3, 4, and 8). In this calculation, y_4 and y_8 for krypton are taken directly from analyzed gas samples. No krypton is present in stream 1 (the absorber feed liquid). Thus, by material balance:

$$x_3 = \frac{Q_4 y_4 - Q_8 y_8}{Q_3} \quad . \tag{14}$$

Values of Q_4 and Q_8 are presented in Tables 8 and 4, respectively. The absorption factors shown in Table 8 are defined as L/VK (where K is the equilibrium coefficient) and are calculated from the liquid-to-vapor flow ratios (Q_3/Q_4) and the krypton equilibrium ratios given

Table 8. Calculated values for stream Q_3 and Q_4 flow rates and the krypton absorption factors

Experiment number	Q_3 (scfm)	Q_4 (scfm)	Q_3/Q_4	Absorption factor
222	43.52	4.15	10.48	1.29
232	44.94	7.17	6.27	0.81
241	37.10	4.05	9.16	0.90
254	39.32	7.81	5.04	0.72
309	50.14	5.03	9.97	1.15
320	57.58	4.74	12.14	1.43
330	55.74	4.95	11.26	1.32
340	55.79	4.66	11.97	1.43
348	60.38	4.92	12.28	1.45
358	53.58	5.21	10.28	1.23
368	48.50	4.21	11.54	1.41
378	46.82	4.24	11.05	1.42
388	46.92	4.30	10.92	1.40
406	46.84	5.08	9.23	1.34
416	40.75	4.53	8.91	1.30
426	45.37	5.04	9.00	1.19
436	44.19	4.36	10.13	1.33
451	32.99	3.21	10.27	1.27
461	33.31	2.99	11.14	1.42
470	33.58	2.75	12.23	1.55
480	32.84	3.70	8.88	1.07
490	32.80	4.37	7.50	0.92
498	33.54	2.61	12.88	1.58
518	33.18	4.06	8.17	1.26
528	33.11	3.60	9.21	1.40
538	33.38	5.95	5.62	0.87
548	33.11	4.92	6.74	1.02
558	33.03	4.36	7.57	1.13
568	33.28	3.90	8.53	1.32
578	33.19	3.51	9.46	1.41

in Table 7. Measured values of y_4 and y_8, along with calculated values of x_3, are presented in Table 9.

The flow rate of the gas leaving the absorber packed section (Q_6) is found by calculating a material balance around the packed section. Since sampling and analysis of stream 5 (the effective liquid flow to the top of the packed section) indicated little or no evidence of ^{85}Kr, the krypton component balance ignores this stream. Hence, by krypton balance around the packed section:

$$Q_6 = \frac{Q_4 y_4 - Q_3 x_3}{y_6} . \qquad (15)$$

Values of Q_6, along with measured krypton concentrations for streams 4, 6, and 8, are presented in Table 9.

Since at this point in the analysis, stream 4 (i.e., the gas entering the packed section) and stream 6 (i.e., the gas leaving the packed section) are described by flow-rate calculation and krypton concentration measurement, the column DF is found as follows:

$$\text{Column DF} = \frac{Q_4\ y_4}{Q_6\ y_6} . \qquad (16)$$

The column (DF's) are presented in Table 10. Figure 8 presents the variation of column DF with values of L/VK, the absorption factor, evaluated at the lower end of the packed section.

Calculations of HTU's for krypton are based on the following simple and classical equations:[9]

$$\text{HTU} = Z/\text{NTU}, \qquad (17)$$

Table 9. Krypton-85 concentrations of streams 3, 4, and 6 in Campaign II

Experiment number	Measured ^{85}Kr conc. (ppb)			Calculated	
				^{85}Kr conc. (ppb)	Flow rate (scfm)
	Stream 4	Stream 6	Stream 8	Stream 3	Stream 6
222	15.24	0.135	0.088	1.448	2.068
232	16.90	5.770	5.140	2.151	4.248
241	5.18	0.681	0.653	0.488	4.229
254	0.48	0.248	0.214	0.066	4.756
309	32.20	0.228	0.219	3.216	3.243
320	24.30	0.012	0.005	2.001	1.248
330	28.31	0.019	0.016	2.513	2.739
340	26.93	0.014	0.011	2.249	2.246
348	19.11	0.004	0.009	1.556	6.395
358	27.90	0.098	0.090	2.707	3.144
368	22.32	0.011	0.009	1.934	2.524
378	31.15	0.024	0.024	2.816	2.876
388	31.38	0.026	0.025	2.872	2.780
406	19.70	0.057	0.068	2.132	2.492
416	24.00	0.095	0.084	2.688	1.860
426	20.90	0.292	0.281	2.302	3.126
436	16.53	0.069	0.065	1.628	3.052
451	17.41	0.066	0.058	1.690	2.382
461	14.78	0.013	0.016	1.326	2.704
470	15.12	0.013	0.018	1.236	2.409
480	21.80	0.395	0.337	2.421	2.849
490	25.65	3.350	2.810	3.076	3.350
498	12.84	0.005	0.010	0.997	3.222
518	15.83	0.049	0.043	1.936	2.046
528	11.42	0.006	0.009	1.240	2.680
538	18.34	5.490	4.720	2.691	3.496
548	16.10	1.740	1.350	2.256	2.555
558	14.78	0.306	0.238	1.932	2.199
568	13.48	0.038	0.030	1.579	1.669
578	7.35	0.007	0.009	0.776	2.423

Table 10. Mass transfer values for Campaign II

Experiment number	Overall DF	Column DF	Krypton HTU (ft)	Krypton HETP (ft)	Stripper L/V ratio
222	357	227	0.561	0.634	2.59
232	5	5	1.329	1.080	2.60
241	7	7	0.700	0.665	2.60
254	3	3	3.220	2.253	2.25
309	256	219	0.355	0.380	2.73
320	14039	7757	0.383	0.455	2.93
330	4161	2750	0.339	0.388	2.87
340	7000	4139	0.385	0.458	2.86
348	9687	3866	0.348	0.417	3.02
358	619	471	0.380	0.420	2.77
368	7206	3350	0.374	0.442	2.81
378	3214	1927	0.405	0.479	2.80
388	3043	1887	0.400	0.470	2.80
406	1215	704	0.463	0.533	2.76
416	1013	621	0.464	0.527	2.51
426	153	115	0.506	0.549	2.56
436	539	343	0.493	0.566	2.57
451	590	354	0.430	0.483	2.10
461	2602	1267	0.418	0.496	2.09
470	3075	1358	0.482	0.594	1.98
480	87	72	0.345	0.356	2.00
490	10	10	0.588	0.554	2.01
498	5157	2119	0.441	0.549	2.01
518	839	642	0.400	0.447	1.96
528	4038	2455	0.378	0.445	1.99
538	5	6	1.720	1.478	2.00
548	17	18	0.816	0.800	2.02
558	100	96	0.479	0.506	2.00
568	1100	830	0.448	0.512	2.00
578	2908	1543	0.419	0.495	2.01

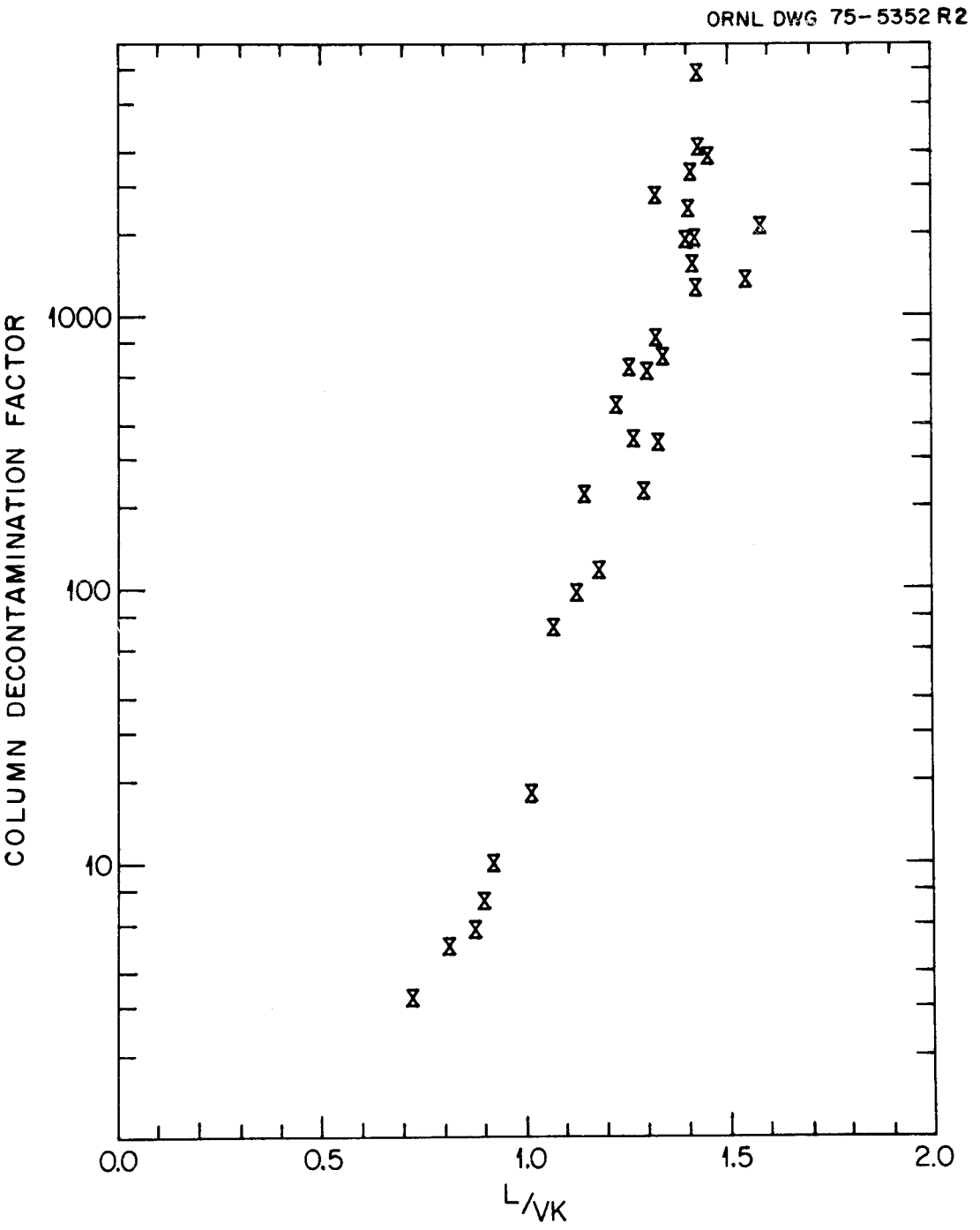

Fig. 8. Decontamination factors vs absorption factors for Campaign II experiments.

$$NTU = \frac{y_o - y_i}{(y^* - y)_{lm}} \quad , \tag{18}$$

$$(y^* - y)_{lm} = \frac{(y_o^* - y_o) - (y_i^* - y_i)}{\ln \frac{y_o^* - y_o}{y_i^* - y_i}} \quad , \tag{19}$$

where

HTU = height of transfer unit, ft,

Z = column packing height, ft,

NTU = number of transfer units,

y_i = inlet gas composition,

y_o = outlet gas composition.

Asterisked quantities (e.g., y_i^*) indicate phase compositions that are in equilibrium with corresponding compositions in the adjacent phase. For present considerations, with all compositions referring to krypton:

$Z = 8.24$ ft,

$y_i = y_4$,

$y_o = y_6$,

$y_i^* = K_i x_3$,

$y_o^* = K_o x_5 = 0$,

K_i = krypton equilibrium ratio evaluated at the temperature of the bottom of the packed section (see Table 7).

Thus,

$$HTU = \frac{8.24\ (y_4 - y_6 - K_i x_3)}{(y_4 - y_6)\ \ln \dfrac{y_4 - K_i x_3}{y_6}}\ \text{ft} . \qquad (20)$$

For each experiment, the value of the temperature calculated for the oxygen-pinched condition at the bottom of the packing (as discussed earlier) is used to evaluate the corresponding value of K_i for krypton for use in Eq. (20). Values of K_i for krypton depend on the system temperature, pressure, and oxygen concentration.[8] Values of HTU calculated by using Eq. (20) are presented in Table 10. Figure 9 illustrates the variation of the packing HTU with column DF.

Values of HETP for each experiment are calculated by using another simple and classical equation:[10]

$$HETP = \frac{Z \ln \dfrac{y_i - y_o}{y_i^* - y_o^*}}{\ln \dfrac{y_i - y_i^*}{y_o - y_o^*}} , \qquad (21)$$

where HETP has units of feet and the other symbols in Eq. (21) are as defined for Eq. (20). For present purposes, Eq. (21) may be rewritten as follows:

$$HETP = \frac{8.24 \ln \dfrac{y_4 - y_6}{K_i x_3}}{\ln \dfrac{y_4 - K_i x_3}{y_6}} . \qquad (22)$$

Values of HETP calculated by Eq. (22) are given in Table 10.

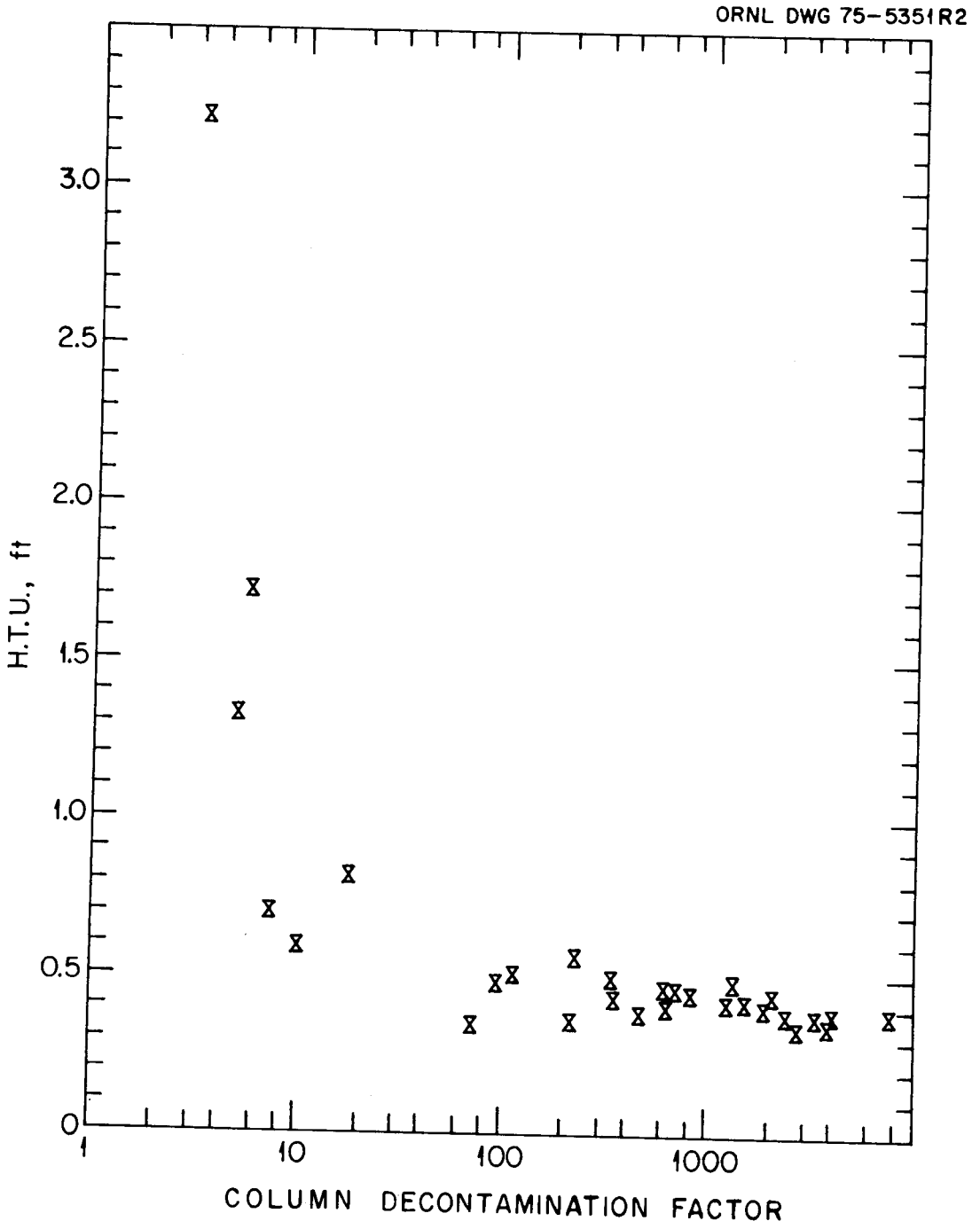

Fig. 9. HTU values for Campaign II experiments.

During Campaign II the stripper column was operated to release all dissolved gases. As noted earlier, little or no detectable solute was found in the purified liquid from the stripper (stream 1). A prime operating characteristic of the stripper to effect this distillation is the liquid-to-vapor flow ratio value. The liquid-to-vapor ratio at the bottom of the stripper was calculated based on the assumption of saturated liquid CO_2 in the reboiler. By material balance around the reboiler:

$$R = \frac{G\,F}{Q\,B} + 1, \qquad (23)$$

where

R = liquid-to-vapor flow ratio in the stripper reboiler, mole/mole,

G = liquid CO_2 pump rate, gpm,

F = flow factor for saturated liquid CO_2 at reboiler temperature, scfm/gpm,

Q = reboiler heat, kW,

B = boilup factor for saturated liquid CO_2 at reboiler temperature, scfm/kW.

Table 10 presents values for R (as the stripper L/V ratio) for each experiment in Campaign II.

5. DISCUSSION

As necessary for clarity, a certain amount of discussion has been included with the experimental and analytical procedures already presented. This section describes the experimental activities of Campaign II in more detail.

5.1 The Experimental Facility

Earlier campaigns and reports concerning the EES-ODF have noted the experimental nature of the facility. The presentation of details for Campaign II should indicate clearly one aspect of this facility. The facility, by design, is intended to provide development data as opposed to demonstration-type information. Development data collected in Campaign II relate specifically to krypton absorption by liquid CO_2. Subsequent campaigns will be concerned with other operations of importance in the KALC process, such as fractionation of lighter gases that are coabsorbed with krypton or complete stripping of all dissolved light gases. Each of these operations is important in the total development of the KALC process, but the EES-ODF is not designed to study all operations simultaneously. The facility is not a prototype KALC system. Rather, it represents an engineering-scale system designed to study individual operations of the KALC process under experimental conditions as closely similar to those expected in an overall process as possible.

Many features of the EES-ODF will undoubtedly have counterparts in a conceptual or subsequent design of the KALC system; however, such features will require technical review for operability, compatibility, and desirability before scale-up to the commercial or semi-commercial system can occur.

5.2 Flooding Studies

The curve shown in Fig. 2 is of the form typically presented[11] as the "generalized" flooding curve except that the usual parameters,

a_p/ε^3, in the ordinate grouping for the particular packing characteristics have been omitted. (Generally, a_p is the total area of packing (ft^2/ft^3 bed), and ε is the void fraction in dry packing.) Moreover, the curve in Fig. 2 only resembles the generalized curve and does not correspond exactly in shape. At any value of the abscissa grouping, the ratio a_p/ε^3 (i.e., the packing factor) can be evaluated by calculating the ratio of the generalized curve ordinate grouping to that of Fig. 2. For example, at a value of the abscissa grouping of unity (near the center of both flooding curves), the packing factor is calculated to be 215 by this method. Hence, in the instance described, the packing of Fig. 2 may be compared to other types as follows:

Packing type	a_p/ε^3	Relative factor
1/2-in. ceramic Raschig rings	428	1.99
5/8-in. polypropylene Pall rings	158	0.73
1/2-in. ceramic Berl saddles	596	2.77
1/2-in. ceramic Intalox saddles	400	1.86
Goodloe wire mesh packing	215	1.00

The relative factors presented above do not necessarily indicate a packing quality or utility higher or lower than the packing used in Campaign II. Many other considerations are important in the selection of packing. Even though much time and effort may be expended searching for an "optimum" material to be used for this purpose, uncertainties will still exist as to whether its performance in practice will be similar to that observed in test equipment. Two important performance considerations here are throughput or capacity and HETP or HTU.

Figure 2 presents evidence that the flooding characteristics of the packing for the 1-1/2-in.- and 3-in.-diam columns are essentially identical for the conditions investigated. Whether identical results will also be obtained in larger-diameter columns is not known. The effect of packing density has not really been determined for the wire mesh packing investigated in Campaign II. Subsequent testing of the larger column (the stripper) in the ORGDP pilot-plant system could shed some light on this matter.

It should be noted that in the event that diameter greatly influences the flooding (and therefore the capacity) in large columns, the use of other "dumped" packings would not circumvent this problem. In fact, the relative size of dumped packing to column diameter may be more difficult to handle for scale-up purposes than considerations of the density of mesh packing.

From the standpoint of capacity, it is likely that the wire mesh packing investigated in Campaign II will provide, within the available time for testing, a reasonable basis for scale-up without undue compromise in mass transfer performance. Also, this material will probably be at least comparable, with regard to capacity, to other commercially available packings.

The question of mass transfer performance is another important consideration when selecting a packing material. Campaign II concerns only absorption in the 1-1/2-in. EES-ODF column. Figure 9 shows that for reasonable values of operational parameters a value of 0.4 to 0.5 ft for HTU results when the procedures discussed in Sect. 4 are used. A number of considerations relating to the accuracy of the

calculational procedures will be discussed later. Of question here is whether the HTU value will vary appreciably with column diameter. Obviously, the question cannot be answered from the Campaign II absorption experiments alone. KALC absorption studies in progress at the ORGDP pilot plant may provide some insight to the problem, but even this information will contain uncertainties relating to (1) wall effects (including heat transfer), (2) sampler effects, and (3) packing density.

Proper distribution of liquid will be important (and require design considerations beyond those for the pilot systems) in the larger-diameter columns. Loading of the column is also important. Other considerations could be mentioned;[11] on the other hand, the result is inevitably that, while various design parameters may be specifically listed, many are not mutually exclusive, and the analytical and engineering translation procedures become very complex. Such is the case for packed column absorption systems in general; and few, if any, of these considerations are related specifically to KALC.

5.3 Equilibrium Operations

Most of the important considerations in equilibrium operations have been discussed previously. At the time the experiments were performed, valid questions existed as to (1) the importance of the equilibrium data accuracy, and (2) the effect of uncertainties in the equilibrium ratios (y/x). Certainly, the data of Notz et al.[4] do exhibit an internal consistency over a relatively large range of

temperatures, and all of their data are reported at essentially infinite dilution. Correlation techniques were used by Mobley[6] to test the apparent consistency with other solutes in liquid CO_2. The net result of the equilibrium operations, together with the finding of Mobley, is that, while the data of Notz et al. are definitely more nearly accurate, a margin of uncertainty regarding absolute accuracy remains.

Just how important it is that the Kr-CO_2 equilibrium values are known to within a given range, say $\pm$ 10%, is not clear. Based on HTU values calculated with Eq. (20), a qualitative relation exists between HTU and K as follows:

$$HTU_2 = HTU_1 \left[\frac{K_2}{K_1}\right]^{-3} . \qquad (24)$$

Consequently, a 10% variation in K (i.e., $\pm$ 5%) would result in a $\pm$ 15% uncertainty in HTU. Such an uncertainty in HTU would not be unacceptable per se; however, the true range of uncertainty would undoubtedly be larger since other factors are known to contribute.

Figure 6 indicates a slightly lower experimental value of $(y/x)_{Kr}$ than one would predict using the data of Notz et al.[4] Mobley's findings via correlations also indicate a slightly lower value and thus tend to fall more in line with other solute behavior in liquid CO_2. Both the equilibrium operations of Campaign II and elements of the correlation work exhibit uncertainties, so that it cannot be stated absolutely that the data of Notz et al.[4] are in error. Finally, although the equilibrium experiments of Campaign II were tedious and time-consuming, perhaps more confidence could be placed

in the results if additional experiments had been conducted. At the present time, however, there appears to be no compelling reason why the data of Notz et al.[4] should not be accepted.

5.4 Mass Transfer Experiments

During Campaign II the independent variable of primary importance was the absorption column liquid-to-vapor flow ration (L/V). Ranges for this and other important variables are summarized as follows:

Variable	Range
Pressure, psig	254 to 409
Temperature, °C	-28.2 to -11.6
Feed O_2 concentration, vol %	5.93 to 20.06
Liquid-to-vapor ratio	
Overall values	4.94 to 12.82
Column only	5.04 to 12.88

Referring to Fig. 7, the overall L/V is Q_1/Q_2, and the column L/V is Q_3/Q_4.

It should be recognized that a 1:1 correspondence does not exist for the above variables over their ranges. That is, the experiment with the highest pressure is not necessarily the experiment with the highest L/V, etc. However, the variables are not totally independent, and a careful review of all variables presented throughout this report is necessary for an appreciation of the nature of the absorption process.

An important observation concerning Campaign II is that variables do behave relative to one another as would be expected based on thermodynamic and chemical engineering principles. In short, no surprises were found. Of equal importance was the considerable operational experience gained, which will be of use in subsequent campaigns and for scale-up design analyses.

The data analysis, as presented earlier, is a major contribution to come out of Campaign II. As noted, the procedures are not always rigorous but, overall, comprise a reasonable set for the specific experiments involved. More precise stream definition is generally desired, and in some cases no stream measurements exist at all. Obviously, future work will need to consider the present analytical procedures, as well as new procedures, when planning new experiments and designing new equipment.

In some ways, the study of absorption may be the least difficult of the studies required (viz., absorption, fractionation, and stripping). However, there are certain similarities among the three studies, and the discussion presented in this report regarding absorption should be applied to future plans for fractionation and stripping experiments.

Considering the data analysis, a note to be emphasized is that the set of procedures used collectively represents a model with all of the usual implications that apply. Most of the calculations pertain to the definition of streams entering and leaving the packed section. In the values of HTU and HETP presented in Table 10, all of the "observed" mass transfer has been ascribed to the 8.24 ft of

packing that is actually present in the absorber in three equal sections of equal length separated by gas and liquid samplers. Four such samplers are present – two between the three sections, and one on each end of the upper and lower sections. No accounting of the mass transfer contribution of the sampler is included in the HTU and HETP values reported since it is not certain exactly what effect should be allowed for. For example, if each sampler is treated as a complete mass transfer unit, then for the 0.4-ft value reported for HTU the corresponding corrected value for the four samplers would be:

$$\text{HTU (nominal, corrected for samplers)} = \frac{8.24}{\frac{8.24}{0.4} - 4} = 0.5 \text{ ft.}$$

The samplers could have a larger or smaller effect than just considered but should not be expected to contribute more than what would be a reasonable safety factor in system design. The 20% effect on HTU just noted is of less concern than the accuracy of the 0.4-ft value itself. If there is some reason to indicate that the HTU values calculated are in gross error [e.g., Eq. (20) is not applicable], then all discussion of the nominal "1/2-ft stage height" is academic.

The few results that indicate appreciably higher values of HTU than 0.4 ft (see Fig. 9) were obtained in essentially pinched experiments, where the HTU equation is erroneously attributing all the mass transfer to the entire packing length instead of to the shorter, effective length. The result is a higher apparent HTU value, and this phenomenon is not unexpected.

The fact that Fig. 8 shows a rather sharp increase in DF as the value of the "absorption factor," L/VK, exceeds unity is indicative of (1) more than just a "few" stages in the absorber, and (2) the "correct" choice of experimental Kr-CO_2 equilibrium data. If only a few stages were present, it would be expected that DF would not increase as rapidly with L/VK. If the data of Laser et al.[3] were correct (or if the data of Notz et al.[4] were grossly in error), the "inflection" of the DF curve of Fig. 8 would not necessarily be at L/VK = 1. Of course, the value of L/V used in L/VK could be in error (it is a calculated value); nevertheless, it is doubtful that the general error associated with L/V would exactly compensate for a corresponding uncertainty in K. Further, since DF (the overall DF is typically a factor of 2 greater than the column DF) is essentially a measured quantity, the ordinate of Fig. 8 can be expected to be indicative of the true situation as far as curve shape is concerned.

6. CONCLUSIONS AND RECOMMENDATIONS

Campaign II provided a wealth of operating experience on which subsequent operations of the EES-ODF can realistically be based. Sampling and analytical techniques appear to be valid and provide a relatively quantitative measurement of composition. However, the absolute accuracy of composition measurements can be evaluated only with additional experimentation.

Flooding performance of the wire mesh packing is reasonably well correlated for the conditions and equipment studied. The krypton

equilibrium data of Notz et al.[4] appear to be sufficiently accurate for experimental purposes of the EES-ODF. For process decontamination factors on the order of 1000, a value of 0.4 ft for the krypton absorption HTU seems realistic and, within the range of the experiments conducted, does not vary for reasonable absorption conditions.

The following recommendations are made as a result of Campaign II:

1. In general, flow rate measurement should be upgraded. Absorber and stripper off-gas rates should definitely be measured.
2. Careful attention should be given to sampling in order to assess the effect on process operations.
3. Continued experimentation should focus on fractionation and stripping processes for the CO_2-O_2-Kr system.
4. The original EES-ODF stripper column should be refitted and installed to allow sampling of the stripper process fluids.
5. In addition to the present capacitance level probes, other means of level measurement should be investigated.
6. More nearly accurate temperature sensors should be sought and tested.

7. REFERENCES

1. R. W. Glass et al., System Features and Component Descriptions for the Unit Operations Off-Gas Decontamination Facility, ORNL-TM-4596 (February 1975).
2. R. W. Glass and H. W. R. Beaujean, Preliminary Fluid Dynamics and Mass Transfer Performance of the Experimental Engineering Section Off-Gas Decontamination Facility Packed Columns, GCR: 74-27 (October 1974).

3. H. W. R. Beaujean et al., "Off-Gas Treatment and Krypton Disposal in HTGR-Fuel Element Reprocessing," presented at the Symposium on the Management of Radioactive Wastes from Fuel Reprocessing, Paris, France, November 27 - December 1, 1972.

4. K. J. Notz, A. B. Meservey, and R. D. Ackley, "The Solubility of Krypton and Xenon in Liquid CO_2" Trans. Am. Nucl. Soc. 17, 318-19 (1973).

5. H. D. Cochran, Jr., and A. D. Ryon, Final Report on the KALC Campaign at the ORGDP Off-Gas Pilot Plant May to June, 1974, GCR: 74-41 (January 1975).

6. R. M. Mobley, "Calculations for the Separation of Radioactive Krypton from the Off-Gas from the Reprocessing of High Temperature Gas-Cooled Reactor Fuel Elements," M. S. Thesis, Department of Chemical Engineering, Clemson University, Clemson, S.C., August 1973.

7. D. M. Levins, R. W. Glass, M. M. Chiles, and D. J. Inman, Monitoring and Analysis of Process Streams in a Krypton-85 Off-Gas Decontamination System, ORNL-TM-4923 (July 1975).

8. R. W. Glass, T. M. Gilliam, and V. L. Fowler, An Empirical Model for Calculating Vapor-Liquid Equilibrium and Associated Phase Enthalpy for the CO_2-O_2-Kr-Xe System for Application to the KALC Process, ORNL-TM-4947 (January 1976).

9. A. S. Faust et al., Principles of Unit Operations, p. 278, Wiley, New York, 1960.

10. W. L. McCabe and J. C. Smith, Unit Operations of Chemical Engineering, P. 606, McGraw-Hill, New York, 1956.

11. R. H. Perry and C. H. Chilton (eds.), Chemical Engineers' Handbook, 5th ed., p. 18-22, McGraw-Hill, New York, 1973.

ORNL-TM-5095
UC-77 — Gas-Cooled Reactor Technology

INTERNAL DISTRIBUTION

1. R. D. Ackley
2. R. E. Barker
3. H. Beaujean
4. R. E. Brooksbank
5. K. B. Brown
6. W. D. Burch
7. W. L. Carter
8. J. H. Coobs
9. F. L. Culler
10. F. E. Dearing
11. R. Eby
12. D. E. Ferguson
13. L. M. Ferris
14. C. L. Fitzgerald
15. C. W. Forsberg
16-20. V. L. Fowler
21. T. M. Gilliam
22-41. R. W. Glass
42. W. S. Groenier
43. P. A. Haas
44. F. E. Harrington
45. D. J. Inman
46-47. P. R. Kasten
48. R. K. Kibbe
49. D. M. Levins
50. K. H. Lin
51. A. L. Lotts
52. L. E. McNeese
53. J. C. Mullins
54. K. J. Notz
55. R. L. Philippone
56. H. Postma
57. A. D. Ryon
58. C. D. Scott
59. J. D. Sease
60. J. W. Snider
61. M. J. Stephenson
62. D. B. Trauger
63. W. E. Unger
64. V. C. A. Vaughen
65. D. C. Watkin
66. M. E. Whatley
67-68. R. G. Wymer
69. O. O. Yarbro
70-71. Central Research Library
72. Document Reference Section
73-78. Laboratory Records
79. Laboratory Records, R.C.
80. ORNL Patent Section
81. W. K. Davis (consultant)
82. J. C. Frye (consultant)
83. C. H. Ice (consultant)
84. J. J. Katz (consultant)
85. R. B. Richards (consultant)

EXTERNAL DISTRIBUTION

86. Research and Technical Support Division, ERDA, ORO
87. Director, Reactor Division, ERDA, ORO
88-89. Director, Nuclear Fuel Cycle and Production, ERDA, Washington, D.C. 20545
90-91. Director, Reactor Research and Development, ERDA, Washington, D.C. 20545
92-253. Given distribution as shown in TID-4500 under Gas-Cooled Reactor Technology category (25 copies — NTIS)
254-291. U.S./German HTR Research Exchange Agreement